6

Design, Sensitivity, and Operation of the TPF Interferometer

The interferometer envisioned for the Terrestrial Planet Finder (TPF) is a complex instrument, particularly in its nulling mode. This chapter and Appendix A summarize some of the technical arguments leading to the choice of a nulling interferometer and introduce some of the issues that define the operation, configuration, and sensitivity of TPF. An illustrative configuration has been selected only to identify critical issues and choices, not to ordain, years in advance of the start of the project, the final design of TPF. The major conclusion of this chapter is that a nulling interferometer operating at 1 AU with four 3.5 m telescopes can detect and characterize Earth-like planets as far away as 15 pc. A smaller system using ~2.5 m apertures could still detect Earth-like planets, but would not be able to search for signs of life, such as ozone, in any but the nearest planetary systems. The illustrative TPF configuration described here will also operate as an imaging interferometer with the sensitivity of the Next Generation Space Telescope (NGST) but with 10 to 100 times the angular resolution of an 8 m filled aperture telescope such as NGST. Since this chapter is necessarily quite technical, non-specialists may wish to skim it or to skip on to later chapters.

INTRODUCTION

The Case for Interferometry. The goal of detecting and characterizing terrestrial planets in the habitable zones of other stars could be achieved in a number of ways. The first variable is the wavelength at which a planet might be detected: reflected light at optical and near-infrared wavelengths, or re-radiated thermal emission in the mid-infrared. A typical star is more than a billion (in the optical) to a million (in the thermal infrared) times brighter than the planet, making the planet undetectable in the star's glare without special efforts to cancel out the starlight (Figure 6.1). This cancellation must operate at the 0.1 arcsec angular separation presented by a 1 AU orbit around a star 10 pc away. We briefly address the instrument concept, filled aperture operating in visible light vs. interferometer operating in the thermal infrared, and conclude that, with the technology we can presently envision and with the goals of characterizing the atmospheres of terrestrial planets, an infrared interferometer is the correct choice.

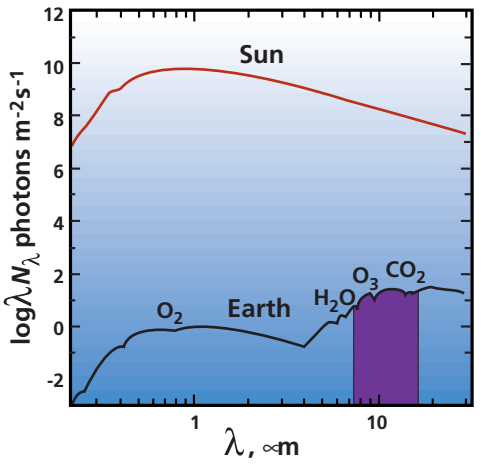

Figure 6.1. The spectral energy distributions of the Sun and the Earth as seen from 10 pc away demonstrate that the intensity ratio problem, while severe in the mid-infrared, is a factor of 1,000 times more favorable than at visible wavelengths. Additionally, the mid-infrared region contains a number of strong, broad spectral features of trace atmospheric gases.

As Figure 6.1 suggests, there are two wavelength ranges to consider for planet searches, visible light or mid-infrared. We examine these in turn:

Visible Light Observations with a Filled Aperture Telescope. The detection of the A-band of molecular oxygen at 0.76 ∝m would be a very exciting result in the search for life on a planet beyond the solar system. Unfortunately, this band is very weak in the Earth's spectrum and the planet-to-star contrast unfavorable. Calculations (Angel and Woolf 1997; Trauger *et al.* 1998) suggest that an ~8 m visible-light telescope with wavefront control of λ/5000 (~0.1 nm) and an advanced coronagraph (Malbet, Yu, and Shao 1995) might detect an Earth-light planet around a star 8 pc away. This level of diffracted and scattered light performance on such a large telescope is well beyond the technology being considered for the Next Generation Space Telescope (NGST). However, the detection of Jupiter-sized planets via direct detection with a coronagraph on NGST is an exciting possibility that should be carefully considered by NASA.

Alternatives to a coronagraph for visible-light observations include placing an inflatable "moon," 100 m in diameter, a few hundred thousand kilometers away from an NGST-class telescope to create an artificial "lunar occultation" that could reveal Earth-like planets around nearby stars (Starkman and Copi 1997). The required inflatable technology is very challenging and would not reach the starlight cancellation level needed to detect an Earth-like planet without scaling the size of, and the distance to, the occulting disk by a factor of ~100.

Thermal Infrared Observations with an Interferometer. As noted in Chapter 4, the mid-infrared band contains numerous molecular lines from trace gases that can be used to assess the habitability of a planet or even to infer the presence of life itself. These lines are deep and broad and could be detectable by low-resolution spectroscopy. The longer wavelengths of mid-infrared radiation necessitate the use of very large apertures or long baselines to resolve the 0.1 arcsec separation of the habitable zone at 10 pc. For example, a coronagraph on a filled aperture telescope typically needs an occulting spot >3 Airy-rings in diameter for effective operation. Thus, a filled aperture telescope with a coronagraph would have to be >25 m in diameter to resolve an Earth analog in the presence of a bright parent star. Such aperture sizes are well beyond extrapolations of NGST technology for filled apertures. On the other hand, interferometers consisting of modest sized telescopes with baselines ~100 m are already under construction or in operation on the ground so that there is a clear technological path (Chapter 12) to a similar space-based instrument.[1]

Thus, from both scientific and technical considerations, the nulling infrared interferometer is preferred for the detection and characterization of terrestrial planets.

Introduction to Interferometry and Nulling. This chapter gives a very brief introduction to nulling interferometry with an emphasis on the factors that determine the sensitivity of TPF. Shao and Colavita (1992) give a general review of optical and infrared interferometry. Woolf and Angel (1998) give a general review of the uses of interferometry for planet detection.

Bracewell and MacPhie (1979) were the first to suggest that a space-based infrared interferometer could suppress the starlight by pointing a null in an interference pattern onto the star while simultaneously detecting the planet through an adjacent bright fringe. To allow the signal from the planet to be distinguished from noise and background sources, they further proposed rotating the array so that the planet signal would be modulated through the fringe pattern at a predictable frequency. Bracewell originally envisaged a rotating two-element interferometer on a rigid structure. Subsequent studies have pointed out that greatly improved sensitivity would be possible using four or more elements with adjustable separations (Angel 1990; Leger *et al.* 1996; the *ExNPS* report 1996; Angel and Woolf 1997). The primary motivation for using more elements is to provide greater starlight suppression. The null should be as broad and deep as possible, but have an angular extent no larger than the orbit of the innermost planet. An interferometer array with more than two elements also offers the potential of fringe patterns with more complicated symmetry to help overcome ambiguities in the image reconstruction. Moreover, if the telescope separations are adjustable, as would be the case in a free-flyer configuration, the restrictions on the shape and width of the null could be relaxed, because the fringe pattern of the array could then be tuned to each candidate star. Mariotti and Mennesson (1997) and Woolf *et al*. (1998) have emphasized the need for an additional level of signal modulation, a technique called "chopping," to suppress light arising from the extended zodiacal cloud around the star and to modulate the desired planetary signals in the face of varying backgrounds and detector drifts.

Images of planetary systems are not formed by direct imaging, but are reconstructed after measurements have been made with the array in

[1]The interferometer concept considered in this report is a Michelson-type device that combines light beams directly to make an interference pattern. An alternative approach would be to use an infrared heterodyne interferometer like the Berkeley Infrared Spatial Interferometer (ISI; Townes *et al.* 1998) which is conceptually identical to interferometers used at radio wavelengths. Heterodyne interferometers offer some practical advantages relative to Michelson interferometers for astronomical imaging (Laubscher, Cooke, and Gisler 1998). However, the intrinsic quantum noise (several $h\nu/k_B$~10,000 K at 10 μm) and narrow bandwidths of present-day heterodyne mixers (~10 GHz) make heterodyne interferometers far less sensitive than Michelson interferometers using broad-band detectors.

multiple configurations. The array is rotated in a plane perpendicular to the line of sight to the star with measurements made at successive position angles. The data consist of a time series of the planet's signal as it rises and falls through the fringe pattern of the rotating array. Despite the lack of complex phase information, images can be reconstructed by cross-correlation (Angel and Woolf 1997; Beichman and Velusamy 1998) or maximum correlation methods analogous to the Fourier transform approach used in synthesis imaging.

The TPF Interferometer. The Terrestrial Planet Finder (TPF) could be implemented in a wide variety of configurations, constrained by the number of telescopes, the necessary degree of starlight and background suppression, and the required accuracy of the reconstructed images. There is a performance trade-off between the ability to provide a deep and wide null to suppress starlight and the ability to chop rapidly to suppress large-scale diffuse emission from a zodiacal cloud. TPF might be designed to have the ability to optimize its performance on-orbit using a number of separate beam-combiner modules. With four telescopes in a linear array, there are a number of possible beam combiners for which the null depth varies with field angle θ according to θ^2, θ^4, or θ^6, depending on how the light is divided and combined from each telescope. The instrument could therefore be reconfigured from one mode to another to optimize the array for each target source.

The choice of TPF configuration will also be driven by the requirement to make high dynamic range images of complex fields in the nonnulling mode for general astrophysical applications. This requirement results in emphasizing long baselines, broad wavelength coverage, and a wide variety of baselines and orientations for optimum *uv*-plane coverage. A separate imaging beam-combiner, corresponding to an individual focal plane instrument in a conventional telescope, will enable TPF to image faint objects with unprecedented angular resolution.

FACTORS AFFECTING THE SENSITIVITY OF TPF

We now consider high-level details of TPF's design. One illustrative configuration, described in Tables 1.1 and A.3, provides a reference for describing the various elements of TPF. It uses a linear array of four telescopes and can employ chopping depending on the configuration of the beam combiner. The precise configuration of the TPF mission will depend greatly on knowledge gained from experience with interferometers presently in development.

The sensitivity of TPF is determined by a large variety of factors, some relating to the target system, some to the instrument, and some to the observing location. This chapter outlines some of the key tradeoffs and demonstrates that an interferometer using 3.5 m telescopes located at 1 AU can detect terrestrial planets in a few hours, characterize their habitability in a few days, and look for signs of photosynthetic life in

a few weeks. Many different instrument configurations are possible; those described herein are meant to satisfy the key scientific measurement goals. Some of the essential astronomical and instrumental factors affecting the ability of TPF to meet its goals include:

- The size, temperature, and atmospheric composition of the target planet.
- The distance to the stellar system, the luminosity, and the physical size of the star.
- The distribution and amount of material of the zodiacal dust in the target system.
- The inclination of the orbital plane to the line of sight.
- Observatory properties such as the size and temperature of the telescopes and associated optics, interferometer baseline and nulling configuration, pointing jitter, etc.
- Instrument properties such as optical efficiency, detector dark current, depth, and stability of the null.
- Local background due to dust in the solar system at the observing location and in the direction of the target.

Appendix A describes the calculations and lists the parameters used in the simulations in this chapter. Each of these parameters must be evaluated carefully to assess the realism of a particular design. Table 6.1 summarizes these calculations and leads to the following conclusions:

1. The emission from exo-zodiacal dust in the target solar system greatly reduces the influence of observing location on the performance of TPF. If emission from a one solar system zodiacal cloud (1 Zodi, see Chapter 5) fills a telescope beam, it does not matter whether that

Table 6.1. Time Requirements For Various Configurations of TPF to Observe Terrestrial Planets

Science Goal	12 µm observation of an Earth at 10 pc	4×2 m (5 AU)	4×0.85 m (1 AU)	4×2 m (1 AU)	4×2.7 m (1 AU)	4×3.5 m (1 AU)
Detect Planet	Spectral Resolution R=3 Signal to Noise SNR=5	1.4 hr	470 hr	15.3 hr	5.1 hr	2.0 hr
Detect Atmosphere CO_2, H_2O	R=20/SNR=10	2.4 day	–	18.1 day	5.9 day	2.3 day
Habitable? Life? O_3,CH_4	R=20/SNR=25	15.0 day	–	–	–	14.7 day

surface brightness arises locally within our solar system, or from the dust cloud surrounding the target star. For example, adding the photon noise produced by the exo-zodiacal signal from a 1 Zodi cloud increases the required collecting area of a 5 AU interferometer by a factor of two to make an observation to a particular sensitivity in a given time, e.g. from 1.5 m mirrors to 2.2 m mirrors. On the other hand, adding in the noise from a 1 Zodi cloud increases the required collecting area of a 1 AU system by only 20% (e.g. from 3.2 m to 3.5 m).

2. A four element interferometer using 3.5 m telescopes operating at 1 AU can achieve a signal-to-noise ratio *SNR*=5 on an Earth-like planet at 10 pc in 2 hr of integration time at a spectral resolution *R*=3 (Table 6.1). This assumes the target system is surrounded by a 1 Zodi cloud.

3. Modest spectral resolution (*R*~20) can be used to characterize the atmospheres of detected planets in longer, but still credible integration times. A spectrum of *R*=20 at *SNR*=10, enough to detect CO_2 and H_20, would take just 2.3 days. A *SNR*=25 spectrum at *R*=20 needed to detect O_3 would take 15 days.

4. Higher spectral resolution and sensitivity than are currently feasible would be required to detect terrestrial levels of other indicators of biological activity such as CH_4 or N_2O (*R*~1000). However, other ecosystems could have far different line strengths than terrestrial so the TPF design should not preclude the ability to find lines throughout the thermal IR spectrum.

Figure 6.2 summarizes the sources of noise and the signal from the planet in a typical TPF observation. The figure shows the strength of the local and exo-zodiacal emission, the leakage from the nulled star, and the background from the 35 K telescope. The resultant signal-to-noise ratio is shown on the right-hand scale.

Table 6.1 compares a broader range of possible interferometers. While a system consisting of SIRTF-style 0.85 m mirrors could barely detect planets at 10 pc, it could detect 1-2 $R_\oplus$ planets at 5 to 8 pc in a few hours to a few days, although without adequate sensitivity to obtain useful spectral information. A 1 AU system consisting of 2.7 m NGST mirror segments could detect broadband emission from an earth at 10 pc in ~6 hours and even offer simple characterization of CO_2 and H_2O in a week. Such a system is a possible fallback if the baseline 3.5 m system cannot be achieved at reasonable cost.

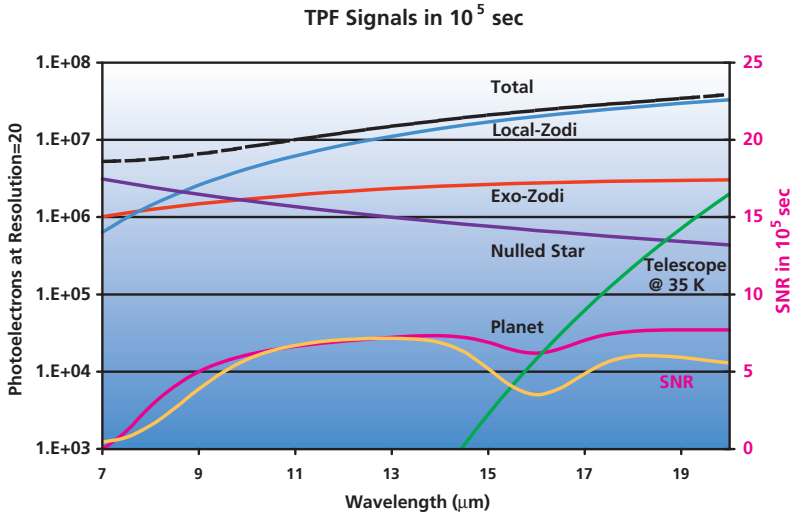

Figure 6.2. The signal in photo-electrons in a 10^5 s integration period from an Earth-like planet observed through the 1 AU, 3.5 m version of TPF. The planet shows CO_2 absorption at 16 μm. The spectral resolution is R=20 and other parameters are as given in Appendix A. Also shown are the other signals that contribute to the total photon shot noise. The bottom curve shows the signal-to-noise ratio (SNR) on the planet using the right-hand scale.

SIMULATIONS OF PLANET DETECTION WITH TPF

By evaluating the interferometer pattern as a function of position angle, it is possible to simulate TPF signals for a variety of interferometer configurations and target planetary systems. Figure 6.3 shows a simulation of a face-on exo-zodiacal cloud and then the cloud as viewed through the interferometer fringe pattern. As the interferometer is rotated around the line-of-sight to the star, a planet goes in and out of the fringe pattern producing a variable signal as shown in Figure 6.4. This TPF data stream can be turned into an image using a number of numerical techniques (Maximum Entropy, CLEAN, etc.) We have used the Maximum Correlation Method (MCM; Aumann *et al.* 1990) using different observing strategies in the presence of zodiacal dust, and with various inclination angles, to investigate the ability to find a planet. Figure 6.5 shows reconstruction of a terrestrial planet (1 $R_\oplus$ at 1 AU) using an increasingly rich set of baselines and wavelengths. The reconstruction shows a few artifacts, a doppleganger on the opposite side of the star and an aliased planet at twice the orbital distance, that can be removed with more sophisticated data acquisition (chopping) and image processing strategies. Figure 6.6 shows a progression of images for a system consisting of Venus, Earth, and Mars as viewed from 10 pc away at an inclination angle of 30°. Venus and Earth are quite prominent, while Mars is below the threshold of detection. All these images were produced using R=20 spectral resolution with a total integration time of 10^6 sec. Figure 6.7 shows a simulated spectrum as would be observed after 15 days of integration.

THE ROLE OF CHOPPING

Low-frequency detector noise, and electronics or thermal background drifts will reduce TPF's sensitivity to the desired signal that results as TPF rotates and sweeps planets across its interference pattern. A tech-

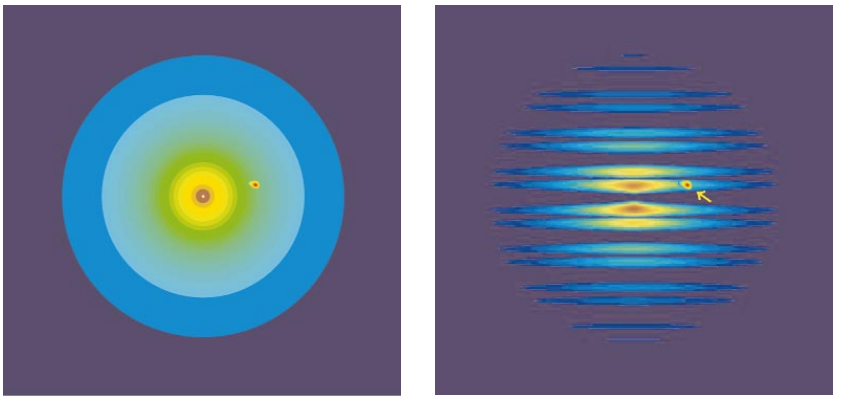

Figure 6.3. The emission from a face-on exo-zodiacal dust cloud (left) with a single planet, and as it will be measured through TPF's transmission pattern (right).

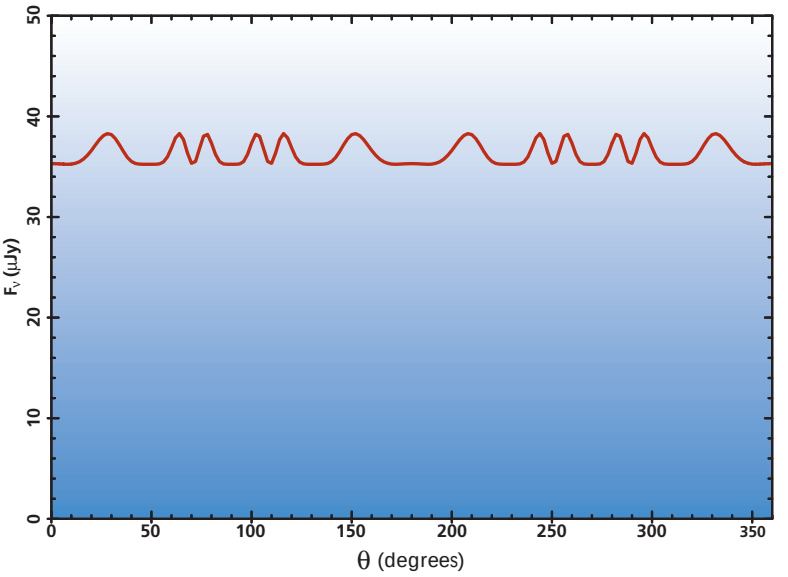

Figure 6.4. As TPF rotates around the line of sight to a target star, the planet (a 3 $R_\oplus$ planet is shown for clarity) produces a modulated signal as it moves in and out of the interferometer fringe pattern. TPF would produce ~20 such data streams, one for each of the observed wavelengths, that would be combined to reconstruct an image of the solar system and the spectra of any detected planets.

nique called chopping, used in both infrared astronomy and radio astronomy, can overcome this problem. If the desired signal can be deliberately modulated (chopped) at a frequency that no other signal is likely to mimic, then a chopped planet signal will systematically average to a steady value while the drifts will tend to average to zero. With TPF, the chopping frequency is set by the minimum readout time of the detector, such that the readout noise remains much smaller than the detected photon flux. For the TPF configuration considered here and in Appendix A, the instantaneous photon rate exceeds a few hundred photo-electrons per second, so that an on-off cycle can occur once per second, far faster than the many-hour rotation period of TPF.

There are a number of configurations for an interferometer than can be used to provide both nulling and chopping. For a fixed number of tele-

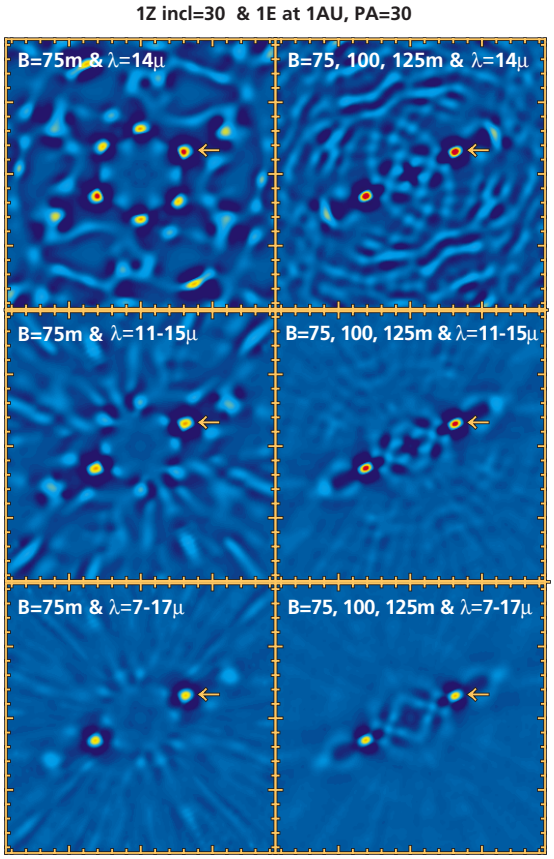

Figure 6.5. A reconstruction of a TPF observation of a terrestrial planet 10 pc away showing improved performance as more wavelengths and baselines are included in the reconstruction.

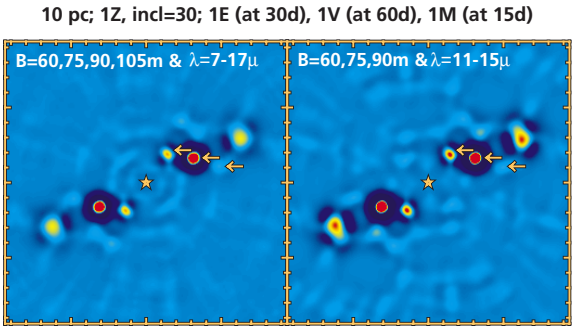

Figure 6.6. A reconstruction of a planetary system at 10 pc containing Venus, Earth, and Mars analogs. The arrows show the positions of the planets. The image artifacts can be removed with more advanced data acquisition and processing.

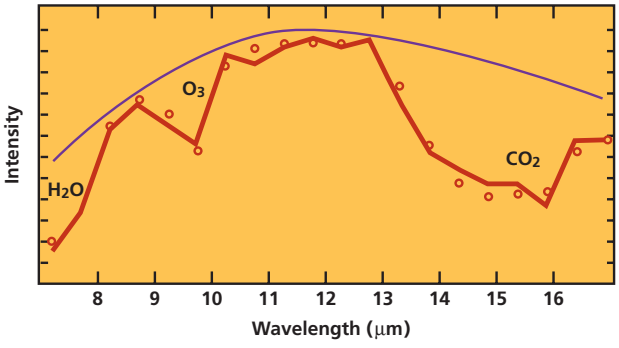

Figure 6.7. A simulated spectrum as would be observed by TPF after ~15 d of integration.

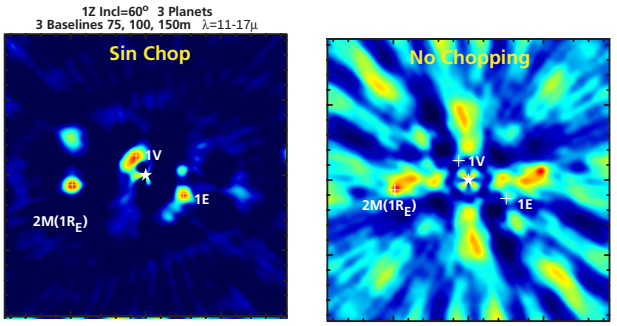

Figure 6.8. A simulation of the Earth-Venus-Mars system seen at an inclination of 60° showing the advantages of a chopped configuration in the presence of bright exo-zodiacal emission. The right figure uses the standard OASES linear array. The left image uses a modified four-element system that uses asymmetric chopping to reject symmetric emission from a zodiacal cloud.

scopes, the chopping comes at the expense of null depth, but the reduced requirements on overall stability make this a very reasonable trade. In some configurations, the planet signals from one set of transmission fringes will turn on while the other alternate set turn off so that the chopped signal reveals whether there is a planet on the left or right hand side of the star. Additionally, the component of zodiacal dust signal that is symmetric about the star is invisible in the chopped signal, because as the signal is turned on from one side of the star, it is turned off on the other side. Figure 6.8 shows how chopping can also reduce the influence of symmetric, diffuse noise sources like the exo-zodiacal emission.

INTERFEROMETER CONFIGURATIONS FOR TPF

The current concept of TPF using four free-flying telescopes offers a wide variety of configurations that could be produced by simple changes of the beam combiner instrumentation and that can be optimized for individual stars. The modes offering the deepest null are the 1:2:2:1 or 1:3:3:1 OASES configurations that can be used for a θ^6 null without chopping.

A number of chopping modes are possible with a four-mirror system. In one chopping mode, the four separate mirrors can alternately serve as parts of two 3-mirror interferometers with a θ^4 null. For the nearest stars, where planet signals may be sufficiently large that chopping is not needed, the system might be configured to give the widest possible null for the lowest possible leakage. For example, merely by taking the same configuration used for Figure 6.9a and by combining the two telescope pairs with a 90° phase shift instead of a 180° shift, it is possible to obtain a null depth that varies as θ^4 but which offers the advantages of rapid chopping.

Table 6.2. TPF Nulling Configurations

Number of telescopes	Array Configuration	Null Width	Chopping
4	Linear 1:2:2:1 or 1:3:3:1	θ^6	No
4	Two 3-Element Interferometers	θ^4	Yes
4	Double Bracewell	θ^2	Yes
4	Angel Cross	θ^4	No
6	Two Fixed, 3-Element Interferometers on Separated Spacecraft	θ^4	Yes
6	ESA's Mariotti Configuration	θ^4	Yes

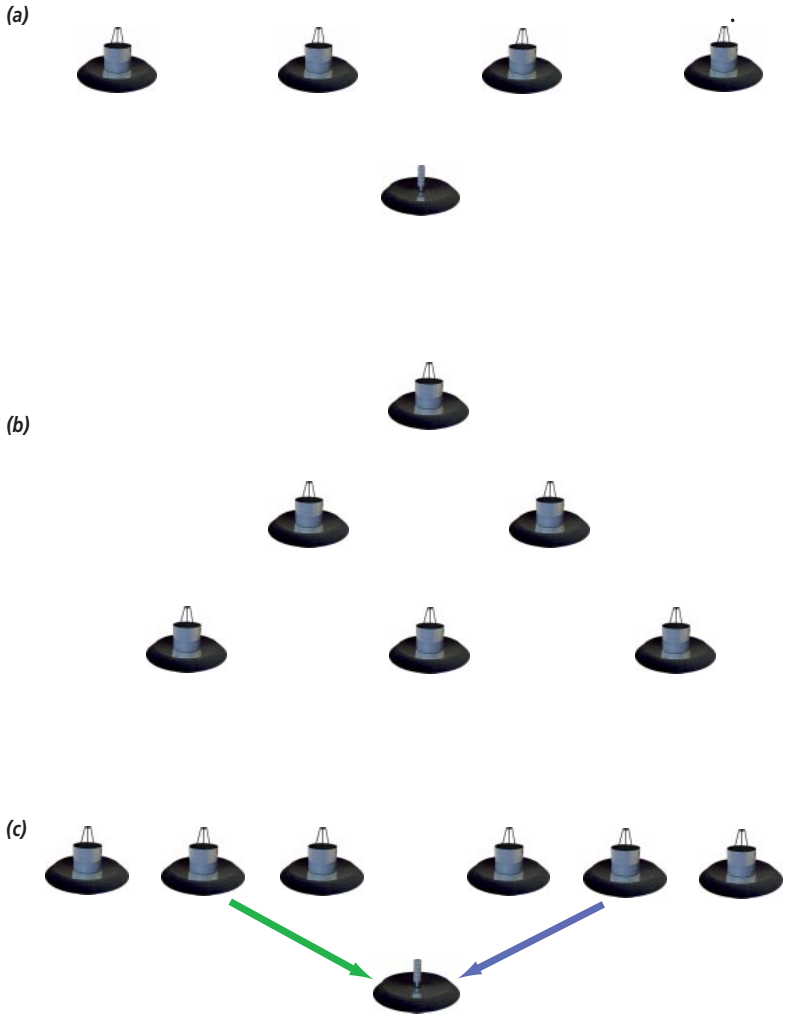

Figure 6.9. Sample interferometer configurations with and without chopping.
a) Nominal OASES or Double Bracewell, with or without chopping;
b) ESA's Marriotti (3DAC) array, with chopping;
c) Dual 3-element, with chopping.

Figure 6.9c illustrates yet another configuration for TPF using a pair of 3-mirror interferometers. Each 3-mirror interferometer provides a θ^4 nulled beam using a fixed ~40 m baseline on a connected boom and is carried on a single spacecraft. The beams from the pair of 3-element interferometers are combined in a central spacecraft with phase shifts of 0°, 90°, 180°, and 270° to produce two output beams corresponding to the sine and cosine components of the signal. These beams allow the determination of the complex visibility of the nulled image. Figure 6.10 demonstrates a simulation of the Earth-Venus-Mars system seen at an inclination of 60°. Advantages of this configuration include rejection of symmetric zodiacal light and the ability to achieve almost arbitrarily high resolution on the planetary system (determined by the inter-spacecraft separation) without excess stellar leakage since the null width is determined by the baseline of individual 3-mirror interferometers. The system can also distinguish a planet from a clumping

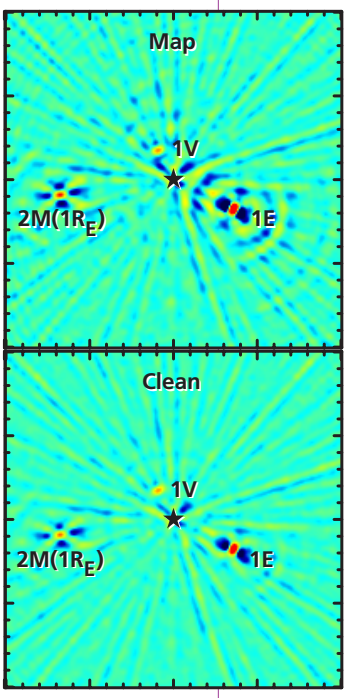

Figure 6.10. A simulation of an Earth-Venus-Mars system (as in Figures 6.6 and 6.8) seen with the system consisting of two fixed-baseline, 3–element interferometers as described in the text. The top image shows an initial reconstructed map. The lower image shows the result of more intensive image processing and should be compared with Figure 6.8.

of zodiacal dust, because the system can resolve low surface-brightness material.

Finally, it should be noted that the European Space Agency Infrared Space Interferometer (IRSI) studies have focused on some very interesting 2-dimensional arrangements of interferometers shown in Figure 6.9b (Mariotti and Mennesson 1998) that offer a different set of advantages (rotation of the array is not required) and drawbacks (needs more spacecraft) from the configurations considered in this study.

The options described here are meant only to illustrate that there are a variety of interferometry configurations that enable nulling at a level adequate to detect planets. This richness of possible configurations, many of which can be compared during flight and tailored to specific stellar systems, is an indication of the robustness of the interferometer design. A great deal of effort will be required over the next few years to arrive at a design that optimizes the performance of the entire system while minimizing cost and complexity.

SENSITIVITY OF TPF FOR GENERAL IMAGING

The high sensitivities that TPF provides for planet detection can also be applied to synthetic imaging. The results in Appendix A can be used to give a conservative estimate of the achievable performance. Under the assumptions in Table A.4, the limiting sensitivity per pixel in a simple reconstructed image is similar to the Earth's flux density at 10 pc, i.e., 0.34 μJy. At a 75 m baseline, this corresponds to a surface brightness of 13 MJy/sr. For longer baselines, with higher interferometric resolution, the corresponding surface brightness is higher.

The imaging sensitivity for an interferometer depends on the surface brightnesses of the source and the background, on the complexity of the source, and on the interferometric resolution. Figure 6.11 shows an illustrative spectral energy distribution for a disk around a young stellar object. The disk is seen in scattered light at short wavelengths and in emitted mid-IR radiation with an integrated 10 μm flux density of 10 mJy. The disk is taken to be 3.8 AU in radius or 25 milli-arcseconds at the distance of the Taurus Molecular Cloud. The figure shows the predicted emission of the disk (red), the strength of the zodiacal and telescope backgrounds (magenta), the signal to noise ratio *per pixel* (black) after a one-day integration at a spectral resolving power of R=100. The number of independent pixels in the image is also indicated based on a maximum baseline of 1 km. The SNR estimates are conservative in that they assume that all points in the image are uniformly bright. Typically a smaller

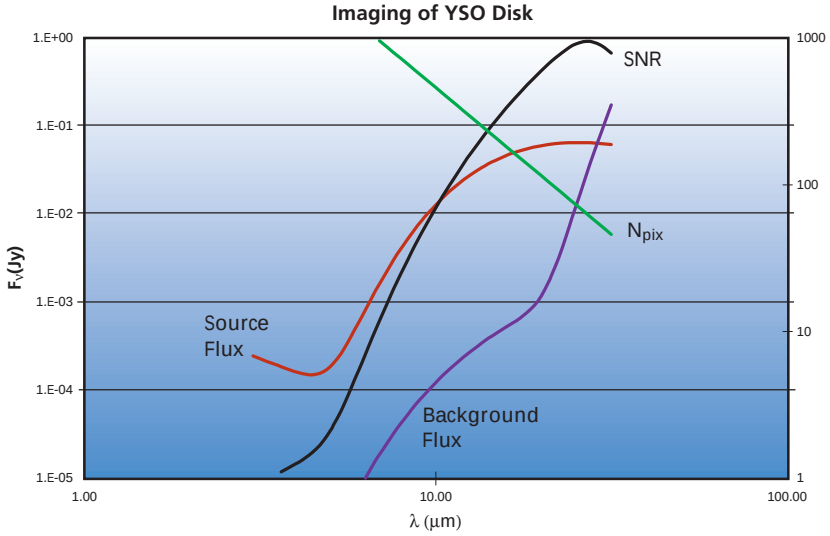

Figure 6.11. Disks around young stars are likely targets for TPF imaging. As described in the text, the figure shows a model for the emission from a disk. Also shown is the background due to the telescope and zodiacal emission. The right-hand scale shows the number of pixels and the signal-to-noise ratio per pixel expected in a TPF map.

number of pixels will dominate the image and be measured with still better signal-to-noise.

For imaging, TPF would use a different back-end instrument than is used for nulling. This imaging combiner would likely be similar to those used for imaging with ground-based interferometers such as the Keck Interferometer. TPF's operational scenario would also be varied from that used for nulling, as described in Chapter 11. The complexity of the object being imaged establishes the array configuration. To first order, the object must be observed on as many baselines as there are interesting pixels in the reconstructed image. These baselines are generated through reconfiguration of TPF's four apertures, radially and azimuthially. The time to achieve this *uv*-plane coverage depends on details of the spacecraft configuration and performance, but will take less than a day to produce excellent, high-dynamic range images.

Achieving high imaging sensitivities with TPF requires stabilizing the interferometer pointing. For the nulling application, there is always a bright central star, which provides sufficient photons for stabilizing the interferometer. For imaging objects with a bright central core, the same source-referenced stabilization scheme can be used. However, in the absence of the bright object feature, an off-axis reference object must be used to stabilize the interferometer. Given the small field-of-view of such a long-baseline interferometer as TPF, the collector telescope assemblies would need to be modified to image and would need to send to the central combiner two fields of view: one containing the science target ($\lambda > 3$ μm) and one containing the reference object ($\lambda <$ 2 μm). The reference object could be as faint as K=17 mag and still serve to stabilize the interferometer on ~ 1 Hz bandwidth needed for imaging with a dynamic range of 100:1. There is typically one such star per square arcminute even at the celestial poles.

APPLICATION OF TPF FOR HIGH SPECTRAL RESOLUTION OBSERVATIONS

For general-purpose imaging observations, TPF will be equipped with delay lines to adjust the path lengths from the telescopes to the beam combiners between an off-axis star and the target object. The delay line range required for off-axis angles of a few arcminutes over a 1 km baseline is about 1 m. However, in addition to providing the delay needed to provide zero path difference for spatial interferometry, the delay line could also be scanned to provide the spectroscopic capability of a Fourier Transform Spectrometer (FTS, e.g. Mariotti and Ridgway 1988). An FTS operating at 5 μm and scanning 1 m would have a spectral resolution of R~200,000 corresponding to a velocity resolution of a few km/sec. By operating with a narrow-band filter to isolate specific spectral lines, e.g. the fundamental band of carbon monoxide or the lines of molecular hydrogen, in the low background conditions of space, TPF would combine milliarcsec spatial resolution, km/sec spectral resolution, and great sensitivity to probe the dynamics of star forming regions.

REFERENCES

A Road Map for the Exploration of Neighboring Planetary Systems (ExNPS) 1996, edited by C.A. Beichman (Jet Propulsion Laboratory: Pasadena, CA), JPL 96-22.

Angel, R. 1990, *The Next Generation Space Telescope*, Bely, P., Burrows, C.J., and Illingworth, G.D. eds. (STScI: Baltimore), p. 81.

Angel, J.R.P. and Woolf, N.J. 1997, *Astrophys. J.* **475**, 373.

Aumann, H.H., Fowler, J.W., and Melnyk, M. 1990, *Astrophys. J.* **99**, 1674.

Backman, D.E., Caroff, L.J., Sanford, S.A., and Wooden, D.H. eds. 1998, *Proceedings of the Exo-zodiacal Dust Workshop*, NASA/CP—1998-10155.

Beichman, C.A. and Velusamy, T. 1997, *Bull. Am. Astron. Soc.* **29**, 1310.

Bernard, J.P., Boulanger, F., Desert, F.X., and Puget, J.L. 1992, *Astron. Astrophys.* **263**, 258.

Bracewell, R.N. and Macphie, R.H. 1979, *Icarus* **38**, 136.

Laubscher, B.E., Cooke, B.J., and Gisler, G.R. 1998, Los Alamos preprint, 98-5917.

Leger, A., Mariotti, J.M., Mennesson, B., Ollivier, M., Puget, J.L., Rouan, D., and Schneider, J. 1996, *Icarus* **123**, 249.

Malbet, F., Yu, J.W., and Shao, M. 1995, *Publ. Am. Astron. Soc. Pac.* **107**, 386.

Mariotti, J.-M. and Mennesson, B. 1997, internal ESA report for the IRSI project.

Mariotti, J.-M. and Ridgway, S.T. 1988, *Astron. Astrophys.* **195**, 350.

Reach, W.T., Franz, B.A., Weiland, J.L., et al. 1995, *Nature* **374**, 521.

Shao, M. and Colavita, M.M. 1992, *Ann. Rev. Astron. Astrophys.* **30**, 457.

Starkman, G. and Copi, C.J. 1997, *Bull. Am. Astron. Soc.* **30**, 764.

Townes, C.H., Bester, M., Danchi, W.C., Hale, D.D.S., Monnier, J.D., Lipman, E.A., Tuthill, P.G., Johnson, M.A., and Walters, D. 1998, in *Astronomical Interferometry*, Reasenberg, R.D. ed., Proc. SPIE **3350** (SPIE Press: Bellingham, WA) p. 908.

Trauger, J., Backman, D., Beichman, C., et al. 1998, *Bull. Am. Astron. Soc.* **30**, 1297.

Woolf, N.J. and Angel, J.R. 1998, *Ann. Rev. Astron. Astrophys.* **36**, 507.

Woolf, N.J., Angel, R., Beichman, C.A., Burge, J., Shao, M., and Tenerelli, D. 1998, in *Astronomical Interferometry*, Reasenberg, R.D. ed., Proc. SPIE **3350** (SPIE Press: Bellingham, WA) p. 683.